PROTEINS: Structure, Function, and Genetics 111–117 (1987)

Three-Dimensional Structure of Neuraminidase of Subtype N9 From an Avian Influenza Virus

A.T. Baker,[1] J.N. Varghese,[1] W.G. Laver,[2] G.M. Air,[3] and P.M. Colman[1]

[1]*CSIRO Division of Protein Chemistry, Parkville, Victoria, Australia 3052;* [2] *John Curtin School of Medical Research, Australian National University, Canberra, ACT, Australia 2601,* [3] *Department of Microbiology, University of Alabama at Birmingham, Birmingham, Alabama 35294*

ABSTRACT **Neuraminidases from different subtypes of influenza virus are characterized by the absence of serological cross-reactivity and an amino acid sequence homology of approximately 50%. The three-dimensional structure of the neuraminidase antigen of subtype N9 from an avian influenza virus (A/tern/Australia/G70c/75) has been determined by X-ray crystallography and shown to be folded similarly to neuraminidase of subtype N2 isolated from a human influenza virus. This result demonstrates that absence of immunological cross-reactivity is no measure of dissimilarity of polypeptide chain folding. Small differences in the way in which the subunits are organized around the molecular fourfold axis are observed. Insertions and deletions with respect to subtype N2 neuraminidase occur in four regions, only one of which is located within the major antigenic determinants around the enzyme active site.**

Key words: crystallography, antigen, glycoprotein

INTRODUCTION

Antigenic variation in type A influenza viruses proceeds by two distinct mechanisms. [1] On the one hand, point mutations in the RNA segments coding for the membrane glycoproteins of the virus, the haemagglutinin and neuraminidase (NA), accumulate under the selective pressure of an immune host population, giving rise to new epidemic-causing strains of virus with annual frequency. On the other, genetic reassortment can result in major antigenic changes to the viral surface proteins and the generation of pandemic-causing influenza strains. In nature, 13 different subtypes of influenza type A haemagglutinin and 9 such subtypes of neuraminidase have been identified.[2] For both neuraminidase and haemagglutinin, serological cross-reactivity may be observed for antigens within a subtype but not between the antigens from different subtypes.

For each of the influenza virus surface antigens, amino acid sequence comparisons between the antigens from within and across subtypes show homologies of around 90% and 50%, respectively. The three-dimensional structures of the hemagglutinin H3 subtype[3] and two neuraminidases of the N2 subtype[4] are known. The latter study on neuraminidases from Tokyo/3/67 (space group I422, a=139.6 Å, c=191.0 Å) and RI/5$^+$/57 (space group $P4_32_12$, a=124.1 Å, c=181.2 Å) demonstrates that antigenic changes within subtypes result in no large-scale perturbations in the protein structure. Indeed, from the level of sequence homology it is to be expected that neuraminidases of different subtypes will also share the same basic three-dimensional structure as that observed for the N2 antigen.

The N2 NA protein is folded into 6 four-stranded antiparallel beta sheets which are arranged as if on the blades of a propeller. The propeller axis is parallel to the fourfold symmetry axis which relates the four subunits in the tetrameric enzyme[4] (Fig. 1). The active site is a pocket lined by amino acids that are invariant in all known strains of influenza and it is encircled by strain-variable loops which are believed to be the antigenic regions.[5] The active site amino acids are Arg118, Glu119, Tyr121, Leu134, Asp151, Arg152, Trp178, Arg224, Glu227, Asp243, His274, Glu276, Glu277, Arg292, Asp330, Lys350, and Glu425.[4] During the course of atomic modeling and refinement of the N2 proteins, the conserved amino acids Asp293 and Arg371 have been found to have their side chains directed toward the active site (J.N.V., unpublished data).

Here we present the first data addressing directly the question of the structures of influenza antigens of different subtypes. The G70c/75 N9 neuraminidase is of particular interest because, when isolated from the virus as rosettes of intact molecules, it has the capacity to agglutinate red cells at 4°C as effectively as H3 haemagglutinin.[6] N2 neuraminidase exhibits no such activity. Neuraminidase of subtype N9 is found to have a very similar three-dimensional structure to the N2 proteins. In all subsequent discussion the amino acid numbering scheme for N2 neuraminidase will be used (for alignment see Fig. 2). As with the N2 NA structural analysis, pronase-solubilized "heads" of neuraminidase, comprising amino acids 80–468, have been used in this study. No atomic structural information is available on the stalk and transmembrane segments of molecules of either subtype.[7]

Received December 30, 1986; accepted May 4, 1987.

Address reprint requests to P.M. Colman, CSIRO Division of Protein Chemistry, 343 Royal Parade, Parkville, Victoria, Australia, 3052.

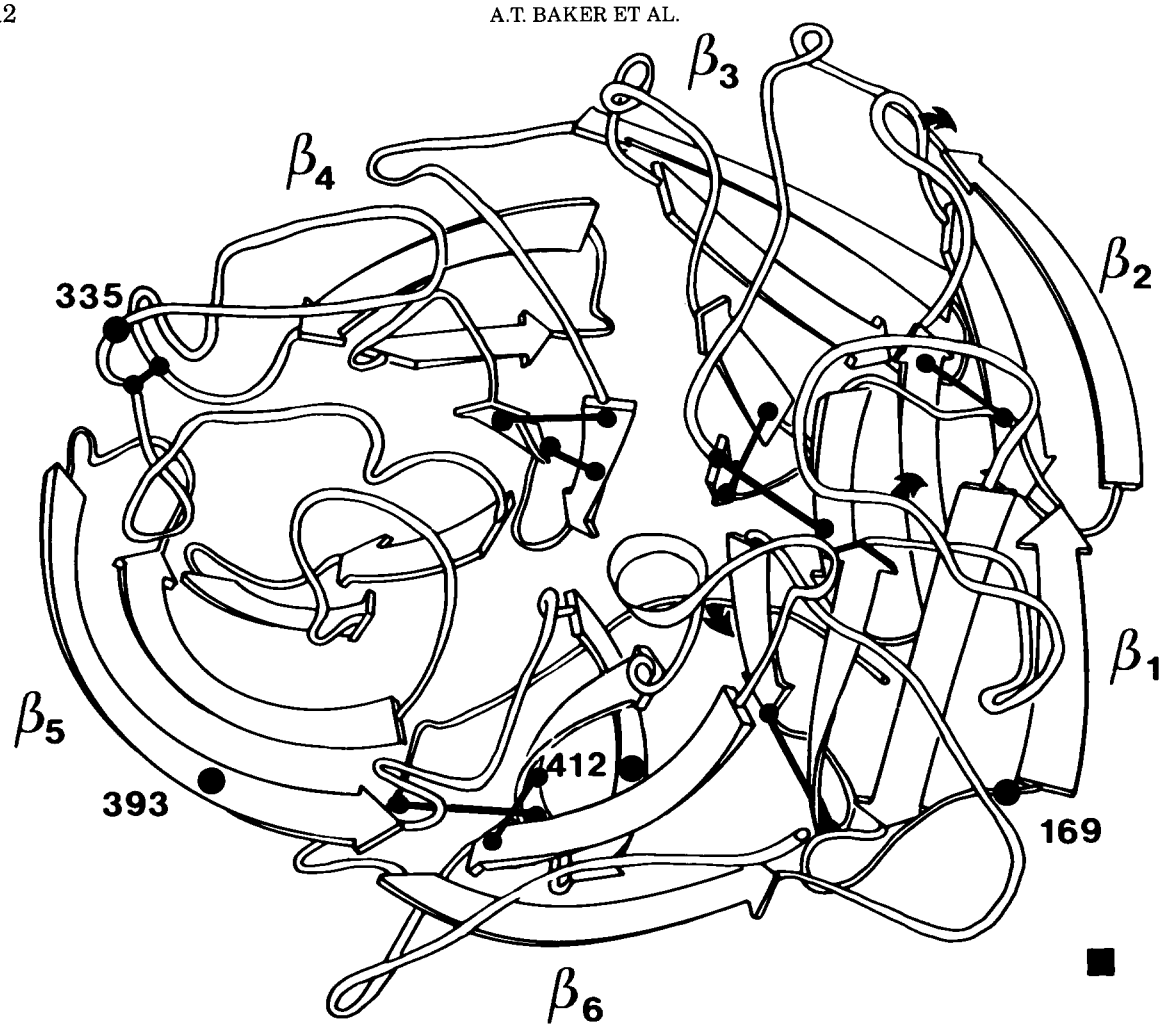

Fig. 1. Diagram of subunit folding of N2 neuraminidase. Positions of deletions (335, 393) and insertions (169, 412) in N9 NA with respect to N2 NA are marked with circles. Bold lines indicate disulfide bonds in N9 NA. Small arrows on the polypeptide chain indicate N9 NA glycosylation sites. The fourfold symmetry axis is normal to the plane of the figure and is marked by the square. In this view, the active site cavity is in the center of the upper surface. The chain tracing in the large loop between beta sheets 4 and 5 is tentative in both subtypes. Schematic diagrams showing the location of antigenic and active site residues can be found in ref. 7.

MATERIALS AND METHODS

Isolation, purification and crystallisation of heads of N9 neuraminidase (N9 NA) from an avian influenza virus G70c/75 have been described previously.[6] N-terminal sequence analysis of pronase-liberated N9 NA heads was by Edman degradation on an Applied Biosystems Gas Phase Sequenator. PTH amino acids were identified by HPLC. Crystals of N9 NA belong to the cubic space group I432 with a=185.1 Å. One subunit of the tetrameric neuraminidase is in the crystallographic asymmetric unit and the molecular fourfold axis coincides with a crystallographic fourfold axis. X-ray diffraction data to 3 Å resolution were collected by oscillation photography around the [110] axis by using a rotating anode source, and films representing scans of 2° were processed by the method and programs of Rossmann[8] and Rossmann et al.[9] The native data is 83% complete to 3 Å. A single heavy atom derivative was prepared by soaking the crystals for 4 days in 10 mM amounts of K_2PtCl_4 in crystallization buffer (1.9 M potassium phosphate, pH 6.8). Heavy atom sites were located in the usual way by difference Patterson and difference Fourier methods. The structure was solved by recognizing that the platinum complex was bound to N9 NA at one site in common with that observed for binding to Tokyo/3/67 NA,[4] namely, at the disulphide of residues 92 and 417.

Data to 3 Å resolution were also collected on crystals soaked in a solution of the neuraminidase inhibitor 2-deoxy-2,3-dehydro-N-acetylneuraminic acid.[10] The crystals were soaked for 4 days in 5 mM amounts of inhibitor in crystallization buffer.

A "stripped-down" version of the Tokyo/3/67 NA molecule was constructed by eliminating the 204 side chains which were not conserved between Tokyo/3/67 NA and N9 NA heads, and this Tokyo/3/67 NA structure was then fitted into the N9 NA crystal by an orthogonal transformation consistent with the heavy atom binding data. Least-squares refinement was in-

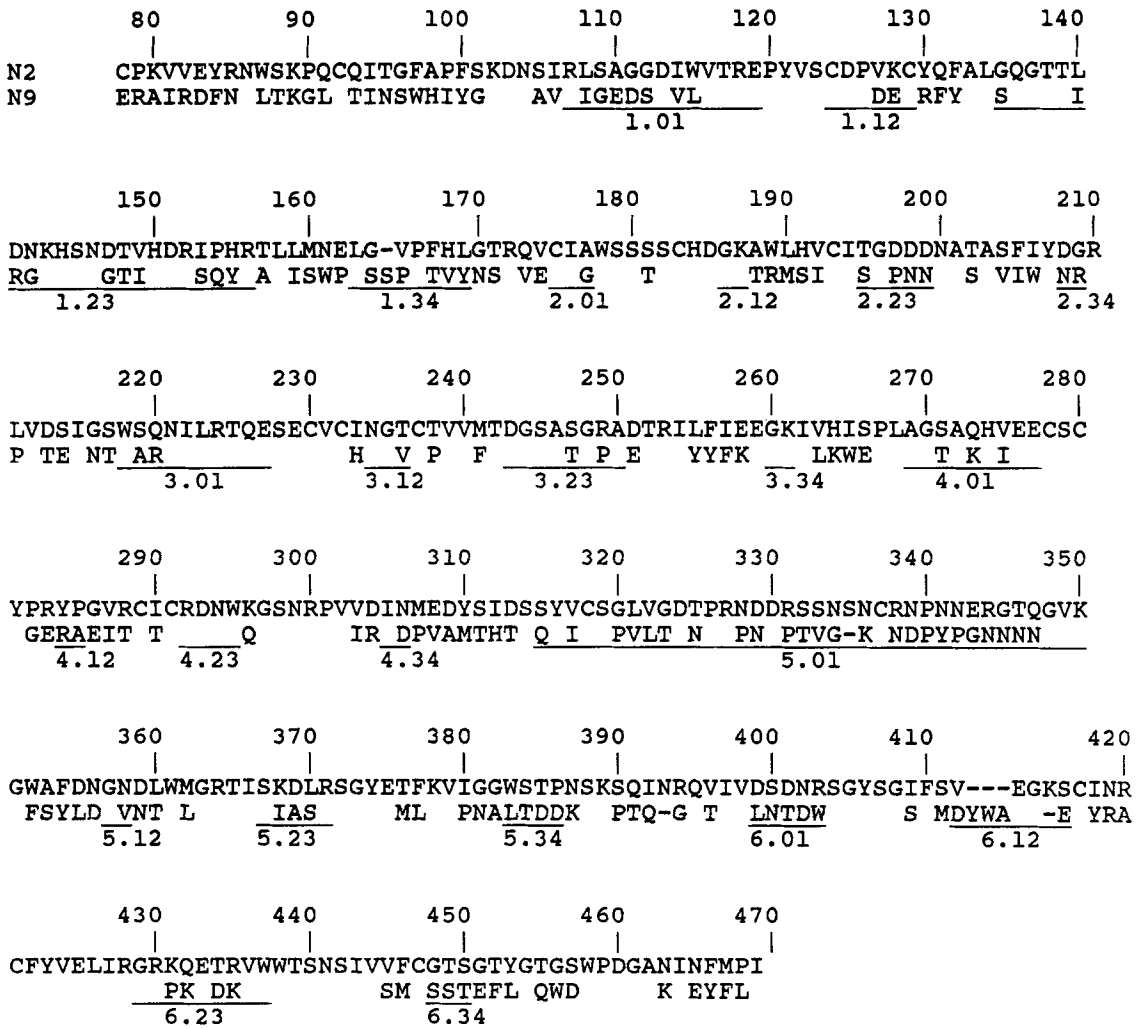

Fig. 2. Alignment of N2 and N9 neuraminidase amino acid sequences. Above: N2 (A/Tokyo/3/67); below: N9 (A/tern/Australia/G70c/75). Homology is indicated by blanks in the N9 sequence; insertions and deletions are indicated by dashes in the appropriate sequence. The positions of the loops between the strands of the beta sheets are shown below the sequences. N.XY (equivalent to $\beta_N L_{XY}$ in the text) indicates the loop between strands X and Y of beta sheet N.[4] Loops N.01 and N.23 are on the top of the neuraminidase head; loops N.12 and N.34 are on the bottom of the head (i.e., toward the virus when the enzyme is membrane-bound). There is little homology in the loop regions of the molecule except where a loop carries amino acids that are within the active site (e.g., loops 1.01, 1.23, 3.01, 4.01, and 4.23).

itiated with CORELS[11] by using the stripped-down Tokyo/3/67 NA structure as the starting model. Low-resolution data, to 15 Å only, were used in the first instance, and the neuraminidase subunit was treated as a single rigid body. At each resolution range five cycles of refinement were performed.

After the final CORELS cycles using data in the 8–5 Å shell, 11 cycles of PROLSQ,[12] at 3 Å resolution, were executed prior to calculation of a $2F_o$-F_c Fourier map for display and modeling with FRODO[13] on an Evans and Sutherland PS300. Following remodeling, a further 33 cycles of PROLSQ were performed and the resulting model is the one discussed in this communication.

RESULTS

The N-terminal sequence of G70c/75 N9 NA heads is AIRDFN–LTK. Pronase has therefore cut the

TABLE I. Data Collection and Merging

Compound	No. of measurements	No. of independent reflections	Rmerge*
Native	29,387	8,500	.115
K_2PtCl_4	18,553	6,404	.128
DDNA†	27,488	8,181	.112

*Rmerge = $\Sigma (I_i - \bar{I}) / \Sigma I_i$, the sum being over all independent reflections.
†DDNA is 2-deoxy-2,3,dehydro-N-acetylneuraminic acid.

TABLE II. Progress of CORELS Refinement

Cycle	Resolution	R-factor*	Correlation coefficient†
1	20–15	.478	.265
2	17–13	.457	.338
3	15–10	.450	.326
4	12–8	.419	.422
6	10–6	.435	.309
11	8–5	.428	.324

*R-factor is $\Sigma \, ||F_o| - |F_c|| \, / \Sigma |F_o|$.

†Correlation coefficient is $\frac{n\Sigma F_o F_c - \Sigma F_o \Sigma F_c}{[(n\Sigma(F_o)^2 - (\Sigma F_o)^2)(n\Sigma(F_c)^2 - (\Sigma F_c)^2)]^{1/2}}$.

Arg79-Ala80 peptide bond.[14] The blank at position 86 corresponds to an Asn in the gene sequence.[14] This Asn is glycosylated in N2 NA[15] and also in N9 NA (see below).

The results of data collection and merging for the native protein, a single heavy atom derivative, and inhibitor-soaked crystals are shown in Table I.

The major heavy atom site is at (.013, .145, .207) and is 26.9 Å from the fourfold symmetry axis (Z-axis). A similarly located binding site for the same compound attached to Tokyo/3/67 NA (low salt) crystals was observed during the course of the structure analysis of the Tokyo/3/67 NA enzyme[4] and is now known to result from binding of the platinum tetrachloride ion to the sulfur atoms in the disulphide linkage between Cys92 and Cys417.

Based on this heavy atom data only two solutions for the structure can be entertained. Modeling of the N9 NA crystal by computer graphics enabled a clear choice between these alternatives for the Tokyo/3/67 NA structure in the N9 crystal. In the one case, serious overlap of molecules occurred near the 432 point group center, whereas in the other, reasonable contacts occurred between neuraminidase tetramers across the plane Z=1/2. Indeed, these latter contacts involving carbohydrate are rather similar to those that occur in crystals of Tokyo/3/67 N2 NA (see below).

A summary of the rigid body refinement is given in Table II. Without the use of very-low-resolution data in the early stages of refinement, the procedure failed to converge to a solution with significant correlation coefficient between F_0 and F_c for the "stripped-down" Tokyo/3/67 NA molecule in the N9 NA crystal. Similar experiences have been reported elsewhere and presumably reflect inaccuracies in the starting model larger than can be overcome by least-squares refinement with high-resolution data only.[16] We also note that the correlation coefficient is a more sensitive measure of the progress of the refinement than is the R factor.[17]

The rigid body transformation which maps the N2 neuraminidase subunit of the Tokyo/3/67 strain from its crystal environment (space group I422, molecular fourfold axis along crystallographic fourfold axis[4]) into the N9 NA crystal reduces to Eulerian angle rotations of −9.0° around the Z-axis, 2.7° around the new position of the X-axis, and −0.2° around the new position of the Y-axis. The center of gravity of the subunit shifts from (15.2 Å, 23.9 Å, 53.9 Å) to (19.2 Å, 21.7 Å, 55.8 Å) in transforming from Tokyo/3/67 NA to N9 NA. The significance of the slightly increased radius (0.6 Å) of N9 NA with respect to Tokyo/3/67 NA is marginal at this stage of the analysis. The Z-axis rotation of 9° is, of course, a parameter of mapping from Tokyo/3/67 N2 NA to N9 NA crystal forms, but the rotation of the subunit around the X and Y axes noted above alters the inclination of the subunit with respect to the molecular fourfold axis. This difference will result in different intersubunit packing around the molecular fourfold axis for the N2 NA and N9 NA proteins and might correlate with amino acid substitutions within the interface between Tokyo/3/67 N2 NA and N9 NA as discussed below.

Further crystallographic refinement obtained by using the Hendrickson-Konnert program[12] has yielded an R-value of 0.32 for data between 6 and 3 Å resolution with standard deviations on bond lengths and bond angles of 0.021 Å and 3.1°, respectively.

Fourier maps with phases based only on the common parts of the Tokyo/3/67 NA and N9 NA structures revealed the location of many of the noncommon side chains together with those minor alterations in chain tracing that accompany the various insertions and deletions in N9 NA with respect to Tokyo/3/67 NA. The two sequences covering the head portions of the molecule are reproduced[14] in Figure 2. The homology is 52%. N2 NA numbering is used to facilitate comparison with the Tokyo/3/67 N2 NA structure and data published previously.[4,5] The alignment given here is only marginally different than that reported earlier.[14] In particular, the insertion in N9 NA of residue 169a (and not 164a) is unambiguous; the additional amino acid, Tyr, is located close to the fourfold axis. The structural alignment of the Tokyo/3/67 N2 NA and N9 NA structures in this region is shown in Figure 3. The $2F_o$-F_c map for N9 NA around residue 169a is shown in Figure 4. The insertion after 308 and the deletion of 314 given in the previous alignment[14] have no basis in terms of sequence homology or structure and have been ignored. The inclusion of Tyr and Trp after 412 has been built as a double insertion rather than as a triple insertion with a deletion of 415[14] but the current map of this region is equivocal. The effect, either way, is to shorten this beta strand in N9 NA with respect to Tokyo/3/67 NA. In the region 315–350, the chain tracing here, as in Tokyo/3/67, must be considered tentative. We cannot therefore formally exclude the possibility of significant conformational differences between Tokyo/3/67 NA and N9 NA in this region. The deletion of residue 393 in N9 NA results in regular beta structure in N9 NA where a beta bulge existed in Tokyo/3/67 NA.[4]

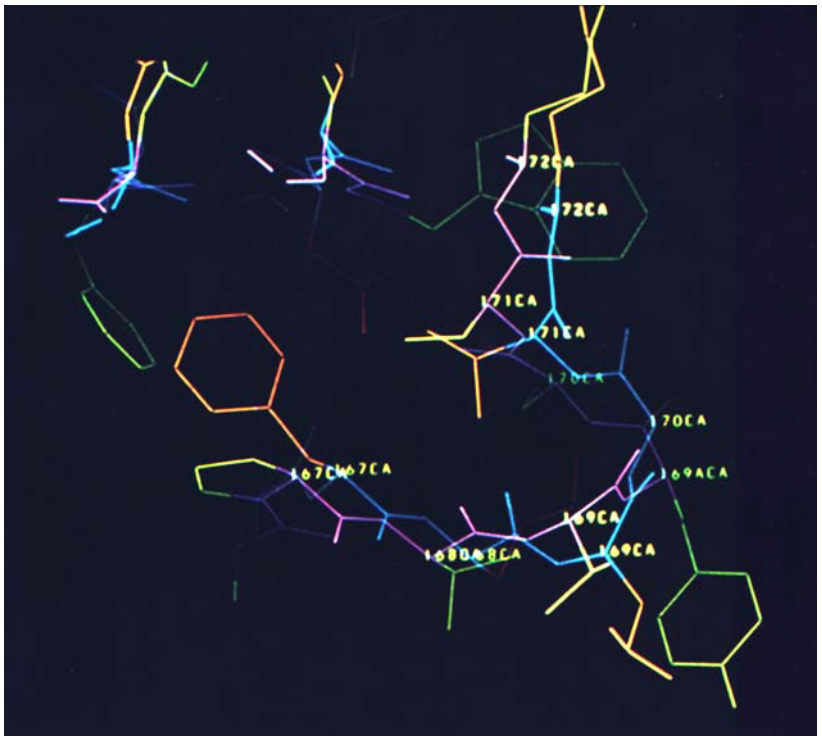

Fig. 3. Spatial alignment of the region around residue 169a. Tokyo/3/67 N2 NA main chain is shown in blue with side chains in orange. N9 NA main chain is shown in purple and side chains are colored yellow-green. Note that the only significant loss of register occurs at residues 169a and 170.

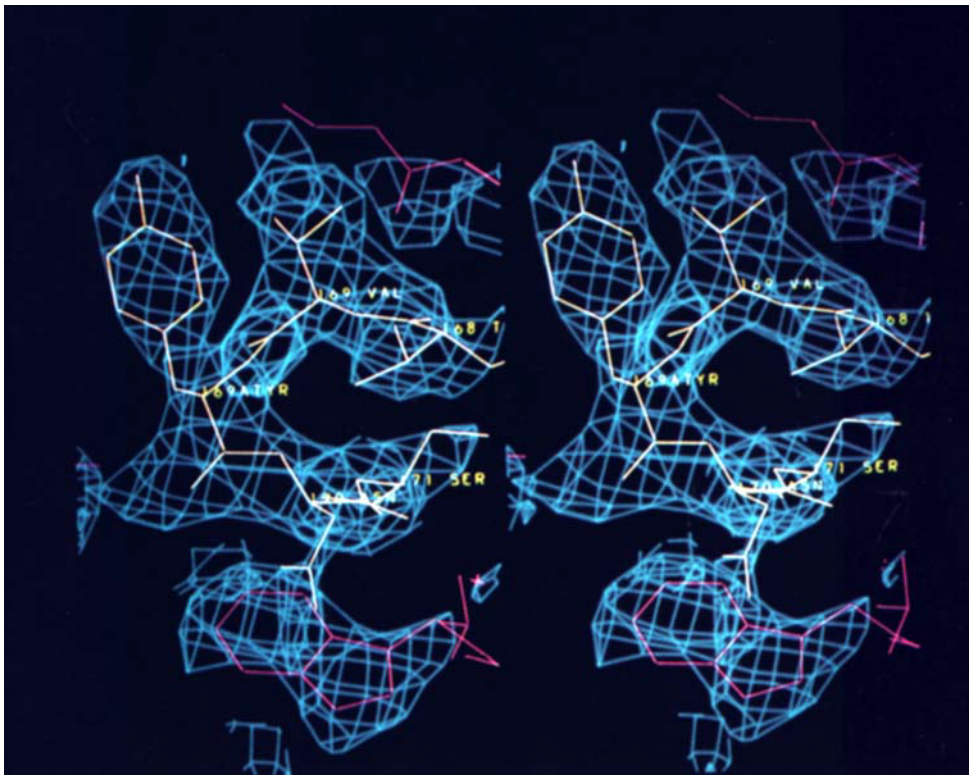

Fig. 4. $2F_o$-F_c map for N9 NA around residue 169a (N2 numbering) with current model interpretation.

Difference Fourier maps calculated with the phases from the last refinement cycle confirmed that K_2PtCl_4 had indeed bound to the sulfur atoms in the disulphide link between residues 92 and 417. No evidence for the binding of the inhibitor 2-deoxy-2,3-dehydro-N-acetylneuraminic acid was observed.

Significant packing interactions occur between subunits related by the threefold axis at the body diagonal of the unit cell where β_3S_4 (i.e., the fourth strand of beta sheet 3) and β_5L_{12} (i.e., the loop between strands 1 and 2 of beta sheet 5) are in contact, the N-terminal strand is in contact with β_3S_4, and β_4L_{12} is in contact with β_4L_{34}. In addition chain segments around residues 336 and 342, both on β_5L_{01}, are in contact via the body-centering operation.

DISCUSSION

The polypeptide folding of the two neuraminidase subtype antigens N2 and N9 is similar, although a detailed comparison and alignment must await completion of the refinement of the two structures. This result is predictable on the basis of amino acid sequence homologies that have been reported for the neuraminidase antigens of influenza virus[7] but must be seen in the context of the failure of antisera to N2 NA antigens to cross-react with N9 NA antigens and vice versa. With neuraminidase there are many conserved structural aspects, including the position of cysteine residues in disulphide bonds and of hydrophobic cores between the 6 beta sheets of the propeller fold.[4] In addition there is the important conservation of enzyme function, the basis of which is the identity of amino acids located within the active sites of the N2 NA and N9 NA proteins. The additional activity of hemagglutination that is a characteristic of the N9 NA protein is discussed below.

The loops of polypeptide chain between strands of beta sheet are regions of considerable variability in sequence, except where a loop has amino acids necessary for the enzyme function (see Fig. 2). The homology for the bottom loops is only 36% (16/44) whereas the homology in the top loops is 49% (63/129), clearly showing the bias introduced by the presence of conserved active site residues on the top loops. Also the outer strand (S_4, following loop L_{34}) of the beta sheets shows major changes between subtypes N2 and N9. The consequence of these amino acid substitutions between N2 NA and N9 NA is that there exist no conserved epitopes that would allow cross-reactions between antisera to the two subtypes. In the case of the lysozyme-Fab complex, the antigen-antibody interface is approximately 30 by 20 Å, with 16 lysozyme residues making contact with 17 antibody residues.[18] A similarly sized epitope has recently been characterized for a neuraminidase-Fab complex.[19]

There is a small but significant difference in the pattern of association of the subunits around the molecular fourfold axis in the two structures. This is in contrast to the finding of identical patterns of association of subunits in two N2 NA structures, RI/5$^+$/57 and Tokyo/3/67.[4] For the two N2 NA proteins, only one substitution is found near the subunit interface and that is Val174 to Ile. N2 NA and N9 NA structures, on the other hand, are observed to have very different amino acids sequences in some parts of the subunit interface. Examples of amino acids in contact across this boundary are Asp127-Arg209 (Val-Gly in N2 NA), His98-Glu174 (Ala-Val in N2 NA), and Gln154-Asp457 (Pro-Ser in N2 NA). In all those cases, there appears to be an increasingly polar aspect to the interaction in N9 NA compared with N2 NA.

A further substantial difference in the subunit interface structure results from the insertion of one amino acid after residue 169 in the N9 NA sequence. The additional residue in N9 NA, Tyr169a, is located close to the fourfold axis and may, in conjunction with the altered subunit contacts detailed above, be responsible for the slight increase in diameter of the N9 NA tetramer with respect to Tokyo/3/67 N2 NA. The details of how, if at all, these substitutions affect the geometry of association in N9 NA subunits into the tetramer must await final refinement of the structure.

The packing interactions between threefold related molecules and between molecules related by the body-centering symmetry operation have no counterpart in crystals of Tokyo/3/67 NA. However, in Tokyo/3/67 NA crystals, carbohydrate contacts mediate packing up the Z-axis (J.N.V., unpublished data) and these same carbohydrate interactions may also be present in N9 NA as the distance between the amide nitrogen of Asn146 and the symmetry-related atom (y, x, 1−z) is 27.9 Å compared with 28.3 Å in Tokyo/3/67 NA.

Asn-X-Ser/Thr triplets are present in N9 NA at three of the four glycosylation sites in N2 NA,[15] the asparagine residues being 86, 146, and 200 (N2 numbering). Although residue 234 is Asn in the N9 sequence, residue 236 is Val: thus one of the two carbohydrate sites on the bottom on the Tokyo/3/67 NA head is not present in N9 NA. Difference Fourier maps reveal that oligosaccharides are attached at each of these locations, though the model does not include any carbohydrate at this stage. It is noted that whereas Asn402 is a potential fifth, but unglycosylated, carbohydrate binding site in N2 NA, residue 402 is Asp in N9 NA.

The failure to observe binding of the inhibitor 2-deoxy-2,3-dehydro-N-acetylneuraminic acid to the crystalline enzyme is probably a function of the high salt environment of the crystals. N-acetyl neuraminic acid (sialic acid) with approximately 2 orders of magnitude less binding affinity for neuraminidase than its 2-deoxy-2,3-dehydro analogue, binds in the active site of Tokyo/3/67 NA crystals where the crystallization buffer is of low ionic strength. Furthermore, that binding was observed when the Tokyo/3/67 NA structure was less advanced than the N9 NA structure reported here. The active site of N9 NA is exposed to solvent and readily accessible to substrates. Experi-

ments are in progress to find a suitable stabilizing buffer for N9 NA crystals so as to enable binding studies to be undertaken.

The hemagglutinating activity of this particular neuraminidase[6] presumably derives either from the creation of a sialic acid binding site in N9 NA or from a modification of the enzyme activity resulting in a longer-lived enzyme-substrate complex. Neuraminidase activity can be inhibited selectively,[6] implying the existence of separate sites. Two aspects of N9 NA which appeared unique from the sequence study[14] were the substitution of a putative active site residue, Asp198 in N2 NA, for Asn in N9 NA, and a cluster of charged groups around the top of the fourfold symmetry axis in N9 NA. The substitution at residue 198 appears to cause no local changes other than the loss of the charge. The side chains at this position in the two structures are nearly superposable.

Apart from the highly charged region around the fourfold axis, another possible binding site for sialic acid is a small pocket adjacent to the active site cavity. At the rear of the pocket is found Thr365, conserved in neuraminidases from all strains of influenza virus that have been characterized to date. The upper part of this pocket includes on its rim the loop 367–370, where sequence changes within the N2 NA subtype are common and where monoclonal variants of neuraminidase show single amino acid changes with respect to wild-type structures.[5,20]

However, recent sequence data on N9 NA variants which show altered hemagglutinating activity[21] implicate a different region of the structure in sialic acid binding. Monoclonal variants at positions 367, 369, 370, 372, and 400 in N9 NA (N2 NA numbering) show no hemagglutinating activity.[21] These amino acids are clustered in space and form a shallow pocket separated from the catalytic cavity by the 367–370 loop.[21] The spatial separation of the sites implied by these observations is consistent with selective inhibition of enzyme activity.

When conditions for allowing reaction of inhibitors and substrates with the enzyme in the crystals are established, binding studies should permit a direct visualisation of the sialic acid binding site(s).

ACKNOWLEDGMENTS

We thank Bert Van Donkelaar for technical assistance and Phil Strike for amino acid sequence data. This work was supported in part by National Institutes of Health grants AI21659 and AI19084. This collaborative project was greatly assisted by provision of international direct-dialling telephone facilities by the Australian Overseas Telecommunications Commission.

REFERENCES

1. Webster, R.G., Laver, W.G.: Antigenic variation of influenza viruses. In: "The Influenza Viruses and Influenza." Kilbourne, E.D., (ed.) New York: Academic Press, 1975:269–314.
2. Webster, R.G., Laver, W.G., Air, G.M.: Antigenic variation among type A influenza viruses. In: "Genetic of Influenza Viruses." Palese, P., Kingsbury, B.W., eds. New York: Springer Verlag, 1983:127–168.
3. Wilson, I.A., Skehel, J.J., Wiley, D.C.: The hemagglutinin membrane glycoprotein of influenza virus: Structure at 3 Å resolution. Nature 289:366–373, 1981.
4. Varghese, J.N., Laver, W.G., Colman, P.M.: Structure of the influenza virus glycoprotein antigen neuraminidase at 2.9 Å resolution. Nature 303:35–40, 1983.
5. Colman, P.M., Varghese, J.N., Laver, W.G.: Structure of the catalytic and antigenic sites in influenza virus neuraminidase. Nature 303:41–44, 1983.
6. Laver, W.G., Colman, P.M., Webster, R.G., Hinshaw, V.S., Air, G.M.: Influenza virus neuraminidase with haemagglutinin activity. Virology 137:314–323, 1984.
7. Colman, P.M., Ward, C.W.: Structure and diversity of influenza neuraminidase. Curr. Top. Microbiol. Immunol. 114:117–255, 1985.
8. Rossmann, M.G.: Processing oscillation diffraction data for very large unit cells with an automatic convolution technique and profile fitting. J. Appl. Cryst. 12:225–238, 1979.
9. Rossmann, M.G., Leslie, A.G.W., Abdel-Meguid, S.S., Tsukihara, T.: Processing and post-refinement of oscillation camera data. J. Appl. Cryst. 12:570–581, 1979.
10. Meindl, P., Tuppy, H.: Competitive inhibition of Vibrio cholerae neuraminidase by 2-deoxy-2,3-dehydro-N-acylneuraminic acids. Hoppe-Seyler's Z. Physiol. Chem. 350:1088–1092, 1969.
11. Sussman, J.L., Holbrook, S.R., Church, G.M., Kim, S.-H.: A structure-factor least-squares refinement procedure for macromolecular structures using constrained and restrained parameters. Acta Cryst. Ser. A 33:800–804, 1977.
12. Hendrickson, W.A., Konnert, J.H.: Stereochemically restrained crystallographic least-squares refinement of macromolecule structures. In: "Biomolecular Structure, Conformation, Function and Evolution." Vol. 1. Srinivasan, R., ed. Oxford: Pergamon Press, 1981:43–57.
13. Jones, T.A.: FRODO: A graphics fitting program for macromolecules. In: "Crystallographic Computing." Sayre, D., ed. Oxford: Oxford University Press, 1982:303–317.
14. Air, G.M., Ritchie, L.R., Laver, W.G., Colman, P.M.: Gene and protein sequence of an influenza neuraminidase with hemagglutinin activity. Virology 145:117–122, 1985.
15. Ward, C.W., Elleman, T.C., Azad, A.A.: Amino acid sequence of the pronase-released heads of neuraminidase subtype N2 from the Asian strain A/Tokyo/3/67 of influenza virus. Biochem. J. 207:91–95, 1982.
16. Sussman, J.L.: Application of refinement constraints and restraints to proteins and nucleic acids. In: "Methods and Applications in Crystallographic Computing." Hall, S.R., Ashida, T., eds. Oxford: Oxford University Press, 1984:206–237.
17. Driessen, H.P.C., White, H.: Molecular replacement and the crystallins. In: "Molecular Replacement." Machin, P.A., ed. Daresbury: SERC Daresbury Laboratory, 1985:89–91.
18. Amit, A.G., Mariuzza, R.A., Phillips, S.E.V., Poljak, R.J.: Three-dimensional structure of an antigen-antibody complex at 2.8 Å resolution. Science 233:747–758, 1986.
19. Colman, P.M., Laver, W.G., Varghese, J.N., Baker, A.T., Tulloch, P.A., Air, G.M., Webster, R.G.: Three-dimensional structure of a complex of antibody with influenza virus neuraminidase. Nature 326:358–363, 1987.
20. Webster, R.G., Hinshaw, V.S., Laver, W.G: Selection and analysis of antigenic variants of the neuraminidase of N2 influenza viruses with monoclonal antibodies. Virology 117:93–104, 1982.
21. Webster, R.G., Air, G.M., Metzger, D.W., Colman, P.M., Varghese, J.N., Baker, A.T., Laver, W.G.: Antigenic structure and variation in an influenza N9 neuraminidase. J. Virol. (in press).